Brownian Dynamics Simulations of Probe and Self-Diffusion in Concentrated Protein and DNA Solutions

John D. Dwyer* and Victor A. Bloomfield
Department of Biochemistry, University of Minnesota, St. Paul, Minnesota 55108 USA

ABSTRACT We have developed a Brownian dynamics algorithm for simulating probe and self-diffusion in concentrated solutions of DNA and protein. In these simulations, proteins are represented as spheres with radii given by their hydrodynamic radii, while DNA is modeled as a wormlike chain of hydrodynamically equivalent spherical frictional elements. The molecular interaction potentials employed by the program allow for intramolecular stretching and bending motions of the DNA chains, short-range Lennard-Jones interactions, and long-range electrostatic interactions. To test the program, we have carried out simulations of bovine serum albumin (BSA) probe diffusion and DNA self-diffusion in solutions of short-chain DNA as a function of both DNA concentration and solution ionic strength. In addition, we report on simulations of BSA self-diffusion as a function of BSA concentration and ionic strength. Based on a comparison to available experimental data, we find that our simulations accurately predict these transport properties under conditions of physiological salt concentration and predict the stronger concentration dependence observed at lower salt concentrations. These results are discussed in light of the nature of the intermolecular interactions in such systems and the approximations and limitations of the simulation algorithm.

INTRODUCTION

Considerable attention has been given in recent years to characterizing the transport properties of concentrated macromolecular solutions. Such studies are of particular relevance to biological systems where macromolecules constitute over 30% by volume of the cytoplasm (Zimmerman and Minton, 1993). Given that most biological reactions require some sort of diffusion-mediated encounter, a significant question is how are such reactions affected by the strong intermolecular interactions that occur in a crowded environment such as the cytoplasm?

Computer simulation techniques have been shown to be an effective means for exploring the effects of molecular interaction potentials on a wide range of systems and problems. The Brownian dynamics simulation technique (Ermak and McCammon, 1978) is particularly well suited to the relatively long time scale of macromolecular transport processes. While Brownian dynamics simulation has been applied successfully to a host of different problems, there have been relatively few attempts to use this technique to study concentrated systems (Van Megen and Snook, 1988).

In this work, we report on the development of a Brownian dynamics algorithm for simulating probe and self-diffusion in concentrated protein and DNA solutions. The interaction potentials in our program allow for intramolecular stretching and bending motions of DNA chains, short-range Lennard-Jones interactions, and long-range electrostatic interactions modeled by the Debye-Hückel equation. Our goal was to determine whether or not this relatively simple set of interaction potentials, and in particular the Debye-Hückel treatment of the electrostatic interactions, could accurately simulate translational diffusion in concentrated solutions of protein and DNA. To test the program, we have carried out simulations on two different systems for which experimental data are available. Specifically, we have simulated diffusion in solutions containing a small number of bovine serum albumin (BSA) molecules in a background matrix of short-chain DNA molecules and in solutions of BSA alone. From these simulations we have computed: (*a*) the effect of DNA concentration and solution ionic strength on the BSA probe diffusion constant; (*b*) the effect of DNA concentration and solution ionic strength on the DNA self-diffusion constant; and (*c*) the effect of BSA concentration and ionic strength on the BSA self-diffusion constant. We find that the results of our simulations are in overall good agreement with the experimental data and that the Debye-Hückel treatment of the electrostatic interactions does afford a reasonably accurate prediction of the ionic strength dependence of these transport properties. These results are discussed in light of the nature of the intermolecular interactions in such systems and the approximations and limitations of the simulation algorithm.

MATERIALS AND METHODS

The hydrodynamic properties of DNA were simulated by modeling the molecule as a wormlike chain composed of spherical beads of radius 15.9 Å as described by Hagerman and Zimm (1981). For the present study, chains composed of 20 beads were used to model DNA of approximately one persistence length. BSA was modeled as a spherical particle with a radius equal to its hydrodynamic radius of 35 Å (Squire et al., 1968).

The Brownian dynamics simulations were carried out using the method of Ermak and McCammon (1978). Briefly, the position of each particle *i* at

Received for publication 1 July 1993 and in final form 10 August 1993.

Address reprint requests to Dr. Victor A. Bloomfield, Department of Biochemistry, University of Minnesota, 1479 Gortner Ave., St. Paul, MN 55108.

**Permanent address:* Department of Chemistry, College of St. Catherine, 2004 Randolph Avenue, St. Paul, MN 55105. ©

0006-3495/93/11/1810/07 $2.00

time $t + \tau$ was computed from the position at time t using the equation

$$r_i(t + \tau) = r_i(t) + \frac{D_i \tau}{kT} \sum_{j=1}^{N} F_j + R_i(\tau), \quad (1)$$

where D_i is the translational diffusion coefficient of particle i, F_j is the direct interparticle force between particles i and j, and $R_i(\tau)$ is a random displacement vector used to simulate solvent-mediated Brownian motion. Consistent with the fluctuation-dissipation theorem, these random displacements are normally distributed with zero mean and variance $\langle R_i R_j \rangle = 2D\tau\delta_{ij}$, where δ_{ij} is the Kronecker delta. In the present work, hydrodynamic interactions were not computed and thus the diffusion coefficients are scalars.

The force field for these simulations consisted of the sum of several terms. Within each DNA chain, bending and stretching were governed by harmonic potentials of the form described by Allison (1986). Specifically, these were given by

$$U_{\text{stretch}} = \frac{h}{2} \sum_{j=1}^{N-1} (b_j - 2a)^2 \quad (2)$$

and

$$U_{\text{bend}} = \frac{g}{2} \sum_{j=1}^{N-2} \theta_j^2 \quad (3)$$

where b_j is the interbead spacing between adjacent beads in the DNA chain, a is the bead radius, and θ_j is the angle between the two virtual bonds connecting beads $j, j + 1$, and $j + 2$. The force constants for these potentials were calculated from the expressions

$$h = \frac{\alpha k_B T}{(2a)^2} \quad (4)$$

and

$$g = \frac{P k_B T}{2a} \quad (5)$$

where α is a dimensionless parameter designed to ensure that the amplitude of the stretching motions are small and P is the persistence length of the DNA. Values of $\alpha = 100$ and $P = 500$ Å were used in all simulations.

In addition to intrachain potentials, interparticle interactions were governed by a short-range Lennard-Jones potential to ensure volume exclusion and a long-range electrostatic potential approximated by the Debye-Hückel equation. The former was calculated using the expression

$$U_{LJ} = 4\epsilon \left[\left(\frac{\sigma}{r} \right)^{12} - \left(\frac{\sigma}{r} \right)^{6} \right] \quad (6)$$

Here, ϵ is the depth of the Lennard-Jones potential well, r is the distance between two interacting particles, and σ is the sum of the radii of the interacting particles. In all of the simulations described below, a value of $\epsilon = 1.0\ k_B T$ ($T = 300$ K) was used, and Lennard-Jones interactions were cut off at a separation distance of $2^{1/6}\sigma$.

Screened electrostatic interactions were calculated using the Debye-Hückel equation

$$U_{DH} = C \frac{e^{\kappa a}}{1 + \kappa a} \frac{e^{-\kappa r}}{r}, \quad (7)$$

where κ is the inverse Debye length, $C = q_i q_j e^2 / \epsilon k_B T$, and ϵ is the dielectric constant of water (80).

For the electrostatic interaction, the net charge on the DNA chains was calculated assuming 80% charge neutralization due to monovalent counterions (slightly larger than the 76% predicted from counter-ion condensation theory (Manning, 1979)), and thus each bead (which models approximately 10 base pairs) was given a charge of −4.0. The net charge on BSA is ionic strength dependent, and a value of −16.0 was used for simulations in 0.1 M salt and −10.0 for simulations in 0.01 M salt (Guéron and Weisbuch, 1980). Since adjacent beads on the DNA chains were already allowed to interact harmonically, adjacent bead pairs were excluded from both the Lennard-Jones and Debye-Hückel interactions.

Simulations of DNA-BSA solutions were carried out in a 700-Å box containing 9 BSA molecules and from 5 to 100 DNA chains of approximately one persistence length as described above. BSA self-diffusion simulations were carried out in a 500-Å box containing from 20 to 260 BSA molecules. Periodic boundary conditions were used in all simulations.

Due to the relatively high particle densities in these simulations, a linked cell algorithm similar to that described by Grest et al. (1989) was used to compute neighbor lists of particle pairs falling within a specified cutoff distance. Cutoffs are generally not used when electrostatic interactions are computed, but since the length of our simulation cell (700 Å for the DNA simulations; 500 Å for the BSA simulations) was much greater than the Debye length for all systems studied, we found that extending the electrostatic interactions beyond an interparticle separation of $2\kappa^{-1}$ only increased the computational time and did not significantly affect the results of the simulation. Thus $2\kappa^{-1}$ was used as a cutoff for all simulations reported here.

In Brownian dynamics simulations, it is important that the time step τ be small enough to ensure that the forces acting on the particles remain essentially constant over the interval τ. Too short a time step, however, increases the computational time for the simulation. For the systems described in the present work, we found that a time step of 20 ps kept direct force changes to less than 10% and still allowed for the overall trajectory lengths needed to obtain probe diffusion coefficients. One-microsecond trajectories (50,000 time steps) gave diffusion coefficients that were independent of time (see Fig. 1).

Self- and probe diffusion coefficients were obtained by computing the mean squared displacement of each molecule's center of mass at time points throughout each trajectory and averaging over all equivalent molecules. All simulations were preceded by an equilibration phase of 250,000 time steps followed by a minimum of 30 trajectories over which particle mean squared displacements were averaged. This procedure resulted in relative uncertainties in the computed diffusion coefficients of less than 10%.

Simulations were carried out on the Cray X-MP-EA at the Minnesota Supercomputer Center. For the largest system studied (100 20-bead DNA chains plus nine BSA molecules) at the lowest salt concentration (and thus the longest cutoff distance) the program used 0.20 cpu s/step. Thus, with 20 ps steps, a 1-μs trajectory required 2.77 Cray cpu h. The program was also implemented on an IBM RS-6000 model 550 workstation, where the same system required 0.45 cpu s/step, or 6.25 cpu h for a 1-μs trajectory.

RESULTS AND DISCUSSION

A series of 1-μs simulations of BSA probe diffusion in DNA were carried out as described above. Fig. 1 shows the mean squared displacement of BSA as a function of time at varying DNA concentrations and at two ionic strengths. All of the results represent an average of at least 30 trajectories. For times longer than 200–300 ns, mean squared displacement of BSA was a linear function of time for all DNA concentrations and at both ionic strengths. However, with increasing DNA concentration and decreasing ionic strength, mean squared displacement is a nonlinear function of time at short times, indicating a time dependence of the probe diffusion coefficient. This behavior is consistent with a time-dependent relaxation of the background DNA matrix (Schmitz, 1990), which is expected to become slower and more pronounced with increasing DNA concentration and stronger intermolecular interactions.

To further assess the validity of our simulation procedure, we have calculated D/D_o for BSA as a function of DNA concentration and compared these results to those obtained

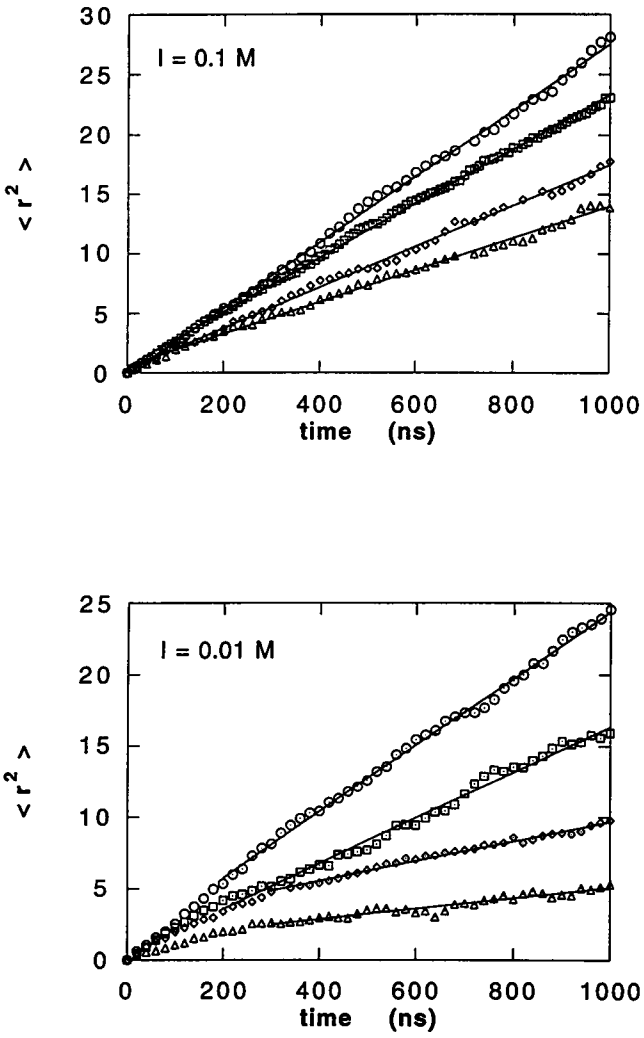

FIGURE 1 Simulated BSA mean squared displacement as a function of time and DNA concentration in I = 0.1 M and I = 0.01 M monovalent salt. [DNA] = 3.0 mg/ml (○), 15.0 mg/ml (□), 30.0 mg/ml (◇), 60.0 mg/ml (△). $\langle r^2 \rangle$ is in units of the BSA hydrodynamic radius squared. Lines are linear least-squares fits of data to $\langle r^2 \rangle = 6Dt$.

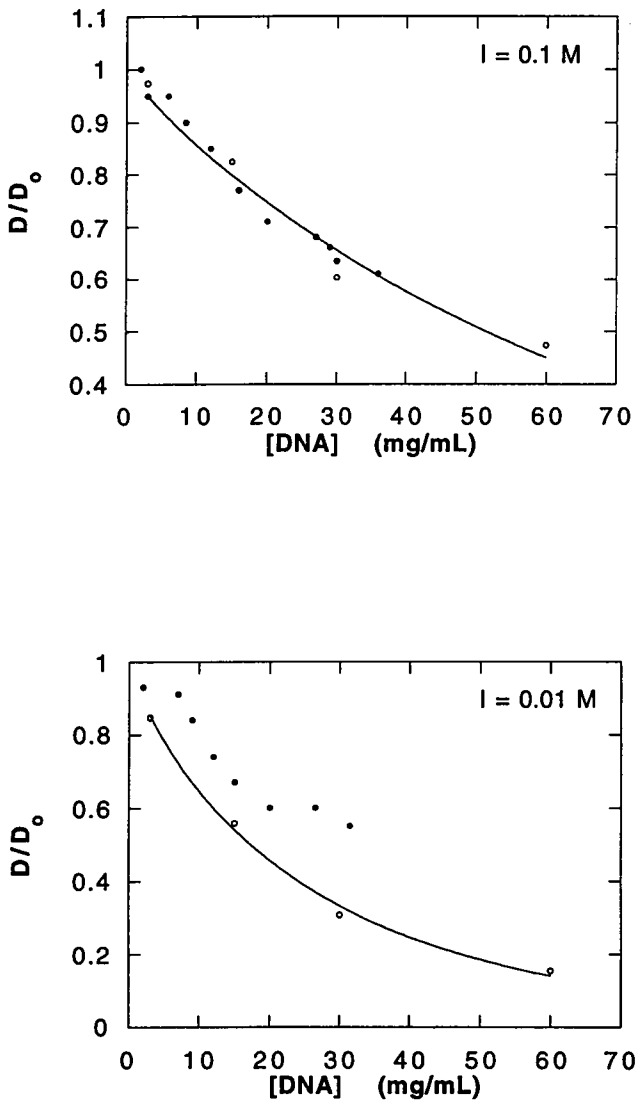

FIGURE 2 Comparison of simulated and experimental probe diffusion of BSA in short-chain DNA in I = 0.1 M and I = 0.01 M monovalent salt. D_o for BSA is 6.37×10^{-7} cm^2/s. (○) simulation; (●) from Wattenbarger et al. (1992). Lines represent nonlinear least-squares fit of simulation data to Eq. 8.

by Wattenbarger et al. (1992), who used fluorescence recovery after photobleaching to characterize the probe diffusion of BSA in solutions of monodisperse, 160-base pair DNA. A value of $D/D_o = 6.37 \times 10^{-7}$ cm^2/s for BSA was calculated using the Stokes-Einstein equation and a value of 35.0 Å for the hydrodynamic radius (Squire et al., 1968). The results of these simulations are shown in Fig. 2. At the higher salt concentration (0.1 M) the simulated results are in good agreement with experiment, whereas at the lower salt concentration the simulation overestimates the effect of DNA concentration on the BSA probe diffusion coefficient by about a factor of 2. Phillies and Peczak (1988) have found that a stretched exponential scaling law of the form

$$D/D_o = \exp(-\alpha c^{\nu}) \tag{8}$$

may be used to describe the concentration dependence of probe and self-diffusion of macromolecules up through the semidilute concentration range. Table 1 summarizes the results of fitting the simulated and experimental BSA probe diffusion data to this equation. In general, the α and ν parameters obtained from the simulation fall within the expected range previously reported for probe diffusion in polymer matrices (Phillies and Peczak, 1988).

The parameters obtained from the high salt simulations are in better agreement with experiment than those obtained at low salt. The reasons for the deviation of simulated and experimental results at low salt are not entirely clear. However, given the relatively simple nature of the interaction potentials used in the simulation, the disagreement is not entirely unexpected. If one uses a more general scaling law of the form

$$D/D_o = \exp(-\alpha' c^{\nu} I^{b}) \tag{9}$$

which includes the ionic strength dependence, our simula-

TABLE 1 Comparison of simulated and experimental stretched exponential parameters obtained by fitting $D/D_0 = \exp(-\alpha c^{\nu})$

Ionic strength (M)	Simulation α	Simulation ν	Experiment α	Experiment ν
BSA probe diffusion in DNA				
0.1	0.019	0.92	0.018	0.95
0.01	0.064	0.84	0.024	0.99
DNA self-diffusion				
0.1	0.016	0.86	—	—
0.01	0.033	0.84	—	—
BSA self-diffusion				
0.1	0.0013	1.28	0.0028	1.14
0.01	0.0086	0.92	—	—

tions give an average b value of −0.477. This compares favorably with the experimental results of Phillies et al. (1989), who reported b values in the range of −0.5 to −0.167 for polystyrene latex sphere probe diffusion in short-chain polyacrylic acid.

Thus it would appear the simple Debye-Hückel interaction potential used in these simulations is able to predict a reasonable ionic strength dependence and that the discrepancy between simulation and experiment at low salt may well be due to other factors. In particular, we believe the absence of hydrodynamic interactions in our simulations is the more likely source of this discrepancy. While the exact nature of the effect of the interplay between direct and hydrodynamic interactions on probe diffusion is unclear, there is theoretical evidence that the two tend to counter or cancel each other to some degree. For example, Hanna et al. (1982) have shown for a hard sphere system that the effect of adding hydrodynamic interactions to direct interactions is to reduce the concentration dependence of self- (probe) diffusion.

We have also computed the concentration dependence of the DNA self-diffusion constant for these same systems, with results summarized in Fig. 3 and Table 1. The simulations show an ionic strength effect with a stronger concentration dependence observed at the lower salt concentration. These simulations are comparable to the experimental data of Wang et al. (1991), who used forced Rayleigh scattering to determine the concentration and ionic strength dependence of the self-diffusion coefficient of 150-base pair DNA fragments. While qualitatively similar, our simulations predict a significantly weaker concentration dependence than is observed experimentally.

While the hard sphere volume fraction of DNA for these simulations ranged from 0.005 to 0.1, interchain electrostatic repulsion is expected to lead to significantly larger effective volume fractions and chain radii. To determine the effective

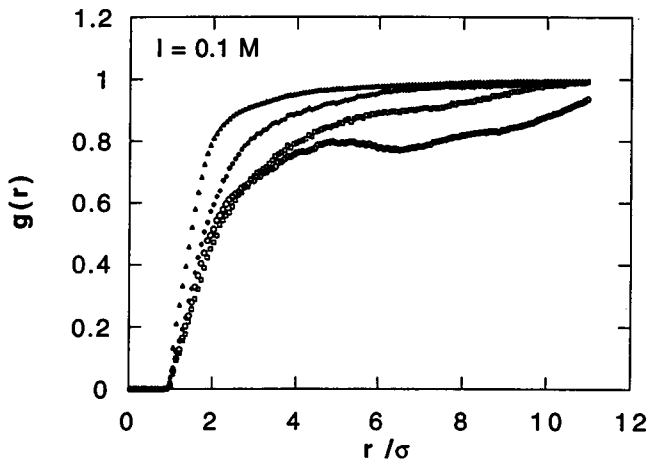

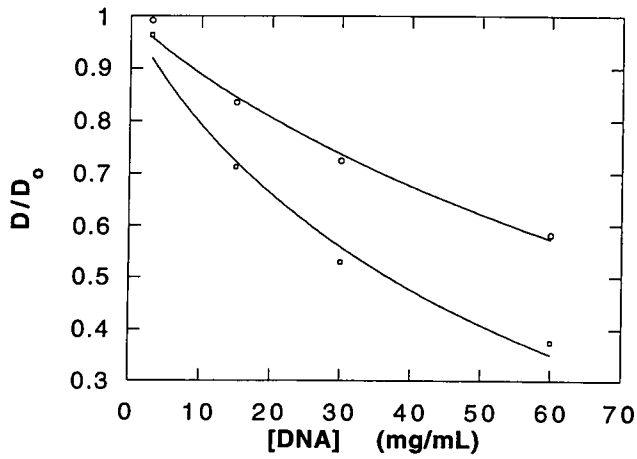

FIGURE 3 Simulation of DNA self-diffusion as a function of DNA concentration and ionic strength. D_o for DNA is 6.91×10^{-8} cm²/s. (○) I = 0.1 M; (□) I = 0.01 M. Lines represent nonlinear least-squares fit of data to Eq. 8.

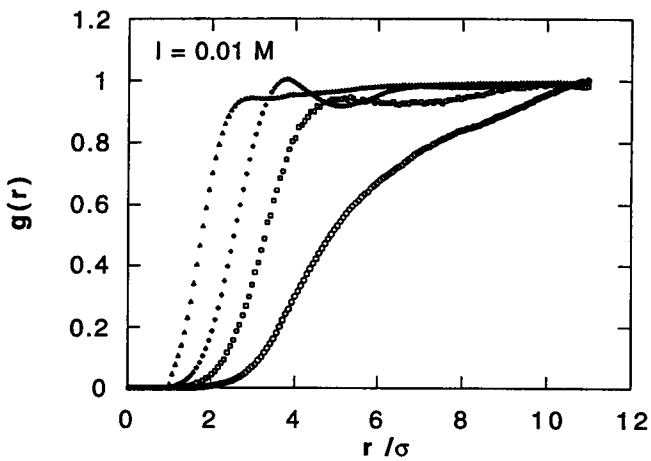

FIGURE 4 Interchain bead-bead radial distribution functions as a function of DNA concentration in I = 0.1 M and I = 0.01 M monovalent salt. [DNA] = 3.0 mg/ml (○), 15.0 mg/ml (□), 30.0 mg/ml (◇), 60.0 mg/ml (△). The diameter (σ) of a DNA bead is 31.8 Å.

size of the DNA chains we have computed the radial distribution functions for interchain DNA bead-bead interactions as a function of both DNA concentration and ionic strength. The results are shown in Fig. 4. Here, r is the computed center-to-center distance between beads on different DNA chains, and σ is twice the hard sphere radius of the DNA beads. The effective radius of the DNA chains was then defined as the value of r/σ at which $g(r) = 0.5$. The results of this calculation are summarized in Table 2. As expected, we find that the effective radius of the DNA chains increases with decreasing ionic strength. The values of r_{eff} obtained here at the lowest DNA concentration (30.8 Å and 77.4 Å at I = 0.1 M and 0.01 M, respectively) are in good agreement with the 28 Å and 78 Å values predicted by Stigter (1977). The concentration dependence of the effective radius, observed most strongly at the lower ionic strength, is a result of packing constraints that force the chains closer together as the DNA concentration is increased. Assuming the DNA chains to be cylinders of radius r_{eff} and length given by $L = (n - 1)\sigma + 2r_{eff}$ where n is the number of beads in each chain (20) and σ is the bead diameter (31.8 Å), we have calculated the effective volume fraction ϕ_{eff} as a function of DNA concentration and ionic strength. As shown in Table 2, these results indicate that at the lower ionic strength, the reduction in r_{eff} with increasing DNA concentration is a result of the need to maintain ϕ_{eff} below the theoretical maximum for close packing.

We have also determined the degree of chain orientational ordering by computing the average of cos θ, where θ is the angle between chain end-to-end vectors. These calculations demonstrate that the DNA chains in all of the systems studied are substantially disordered with $\langle |\cos\theta| \rangle$ values falling in the range of 0.4–0.55. Using an extension of Onsager's theory (Onsager, 1949), Stigter (1979) has shown that charged rods may be expected to undergo a transition from an isotropic to an anisotropic phase with increasing ϕ_{eff}. Recognizing that our DNA chains are not rigid rods, we find that this theory also predicts isotropic solutions for all of the systems studied when we use the r_{eff} values calculated above and limit the rod length to a conservative value of 500 Å.

TABLE 2 Effect of concentration and ionic strength on effective radii and volume fraction as calculated from radial distribution functions (Figs. 4 and 6)

	I = 0.1 M		I = 0.01 M	
	r_{eff} (Å)	ϕ_{eff}	r_{eff} (Å)	ϕ_{eff}
[DNA] (mg/ml)				
3.0	30.8	0.0289	77.4	0.208
15.0	33.2	0.169	52.2	0.442
30.0	28.6	0.248	40.2	0.499
60.0	23.5	0.329	27.8	0.467
[BSA] (mg/ml)				
30.7	42.0	0.0896	57.0	0.217
52.6	42.0	0.149	56.2	0.357
96.4	42.0	0.273	55.4	0.627
140.3	42.0	0.372	47.9	0.589
184.2	41.7	0.514	41.2	0.492

Finally, we have simulated the concentration dependence of BSA self-diffusion with results summarized in Fig. 5 and Table 1. These simulations predict a weak ionic strength dependence that diminishes with increasing protein concentration. Such behavior is consistent with the relatively small size of BSA (Phillies et al., 1989). Most experimental work on this system has been performed at or near the higher salt concentration, and in Fig. 5 we compare the results of our simulations with the experimental results of Muramatsu and Minton (1988), who used fluorescence recovery after photobleaching to characterize the concentration dependence of BSA self-diffusion. The agreement between simulation and experiment is very good. The computed α and ν parameters agree very well with those obtained from experiment and, in fact, are typical of those obtained in most protein self-diffusion studies (Phillies and Peczak, 1988).

The radial distribution functions for BSA obtained from the BSA self-diffusion simulations are shown in Fig. 6. Using the position of the nearest neighbor peak, we have calculated the effective radius and volume fraction of BSA as a function of ionic strength and BSA concentration. These results are summarized in Table 2. As was the case for DNA, we find that the effective size of BSA increases with decreasing ionic strength and at the lower ionic strength is strongly concentration dependent due to packing constraints. The effective radii calculated at the lowest BSA concentrations (42.0 Å and 57.0 Å at I = 0.1 M and 0.01 M, respectively) are in reasonably good agreement with the values of 38 Å and 63 Å predicted by the approximate method of Minton and Edelhoch (1982).

In conclusion, we have shown that a relatively simple Brownian dynamics algorithm is able to accurately simulate probe and self-diffusion in biologically relevant systems at physiological (i.e., high salt) conditions. As such we believe it can be a useful tool for studying the effect of crowding and

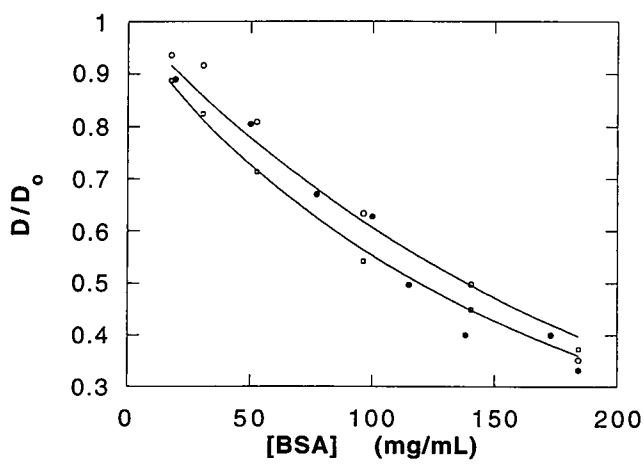

FIGURE 5 Simulated and experimental BSA self-diffusion as a function of BSA concentration and ionic strength. D_o for BSA is 6.37×10^{-7} cm^2/s. (○) simulation in I = 0.1 M monovalent salt; (□) simulation in I = 0.01 M monovalent salt; (●) experimental results from Muramatsu and Minton (1988) in I = 0.1 M monovalent salt. Lines represent nonlinear least-squares fit of simulation data to Eq. 8.

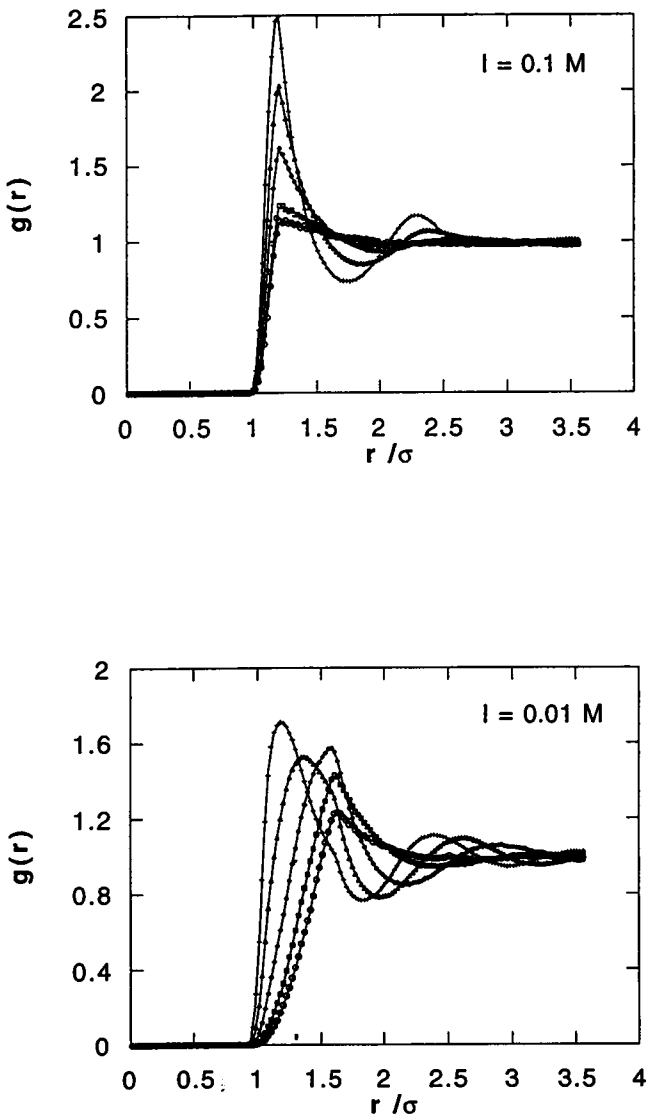

FIGURE 6 BSA radial distribution functions as a function of BSA concentration in I = 0.1 M and I = 0.01 M monovalent salt. [BSA] = 30.7 mg/ml (○), 52.6 mg/ml (□), 96.4 mg/ml (◇), 140.3 mg/ml (△), 184.2 mg/ml (+). The diameter (σ) of BSA is 70 Å.

volume exclusion on macromolecular transport in biological systems. In addition, the program could also be used to study the diffusion of globular synthetic polymers.

A clear limitation of our present program is the absence of hydrodynamic interactions. As noted above, this may explain the observed discrepancies in simulated and experimental results at low salt. However, the inclusion of hydrodynamic interactions in Brownian dynamics simulations of concentrated systems is problematic. Van Megen and Snook (1988) have used an empirically derived pairwise mobility tensor based on the concept of hydrodynamic screening in their simulations of self- and tracer diffusion in charge-stabilized colloidal dispersions. However, while hydrodynamic screening has been theoretically demonstrated for systems containing fixed background particles (Altenberger et al., 1986), detailed hydrodynamic calculations (Beenakker and Mazur, 1984) as well as arguments based on translational invariance (deGennes, 1976) indicate that such screening cannot occur for systems of mobile particles. Furthermore, use of standard two-particle mobility tensors (such as that of Rotne and Prager (1969)) in Brownian dynamics simulations of concentrated systems suffers from two significant problems. First, two-particle tensors neglect the multibody hydrodynamic interactions that are likely to be important in such concentrated systems. Second, while it is possible in principle to implement a multibody mobility tensor (at considerable computational cost), the more fundamental problem is that the linearized Navier-Stokes equation from which hydrodynamic mobility tensors are derived is incompatible with the periodic boundary conditions used in computer simulations (Smith, 1987). The result is that simulations at high particle density quickly lead to configurations that produce a nonpositive definite diffusion tensor. Smith et al. (1987) have derived a periodic mobility tensor that overcomes this problem but at a prohibitively high computational cost for all but the smallest systems. Thus it appears that there is currently no wholly satisfactory means for including hydrodynamic interactions in simulations such as those considered here.

We would like to thank Dr. Ilene Carpenter for many helpful discussions and Professor Norma Allewell and Himanshu Oberoi for access to and assistance in using the IBM RS-6000.

This work was partially supported by National Science Foundation grant DMB9105910. Acknowledgement is made of the donors of the Petroleum Research Fund, administered by the American Chemical Society, for partial support of this research. Supercomputer time was provided under a grant from the Minnesota Supercomputer Center.

REFERENCES

Allison, S. A. 1986. Brownian dynamics simulation of wormlike chains. Fluorescence depolarization and depolarized light scattering. *Macromolecules.* 19:118–124.

Altenberger, A. R., J. S. Dahler, and M. Tirrell. 1986. Hydrodynamic screening and particle dynamics in porous media, semidilute polymer solutions, and polymer gels. *J. Chem. Phys.* 84:5122–5130.

Beenakker, C. W. J., and P. Mazur 1984. Diffusion of spheres in a concentrated suspension II. *Physica A.* 126A:349–370.

deGennes, P. G. 1976. Dynamics of entangled polymer solutions. II. Inclusion of hydrodynamic interactions. *Macromolecules.* 9:594–598.

Ermak, D. L., and J. A. McCammon. 1978. Brownian dynamics with hydrodynamic interactions. *J. Chem. Phys.* 69:1353–1360.

Grest, G. S., B. Dünweg, and K. Kremer. 1989. Vectorized link cell Fortran code for molecular dynamics simulations for a large number of particles. *Comput. Phys. Commun.* 55:269–285.

Guéron, M., and G. Weisbuch. 1980. Polyelectrolyte theory. I. Counterion accumulation, site-binding, and their insensitivity to polyelectrolyte shape in solutions containing finite salt concentrations. *Biopolymers.* 19: 353–382.

Hagerman, P. J., and B. H. Zimm. 1981. Monte Carlo approach to the analysis of the rotational diffusion of wormlike chains. *Biopolymers.* 20: 1481–1502.

Hanna, S., W. Hess, and R. Klein. 1982. Self diffusion of spherical Brownian particles with hard core interaction. *Physica A.* 111A:181–199.

Manning, G. S. 1979. Counterion binding in polyelectrolyte theory. *Accts. Chem. Res.* 12:443–449.

Minton, A., and H. Edelhoch. 1982. Light scattering of bovine serum albumin solutions: extenstion of the hard particle model to allow for electrostatic repulsion. *Biopolymers.* 21:451–458.

Muramatsu, N., and A. P. Minton. 1988. Tracer diffusion of globular proteins in concentrated protein solutions. *Proc. Natl. Acad. Sci. USA.* 85: 2984–2988.

Onsager, L. 1949. The effects of shapes on the interaction of colloidal particles. *Ann. N.Y. Acad. Sci.* 51:627–659.

Phillies, G. D. J., and P. Peczak. 1988. The ubiquity of stretched-exponential forms in polymer dynamics. *Macromolecules.* 21:214–220.

Phillies, G. D. J., T. Pirnat, M. Kiss, N. Teasdale, D. Maclung, H. Inglefield, C. Malone, A. Rau, L-P. Yu, and J. Rollings. 1989. Probe diffusion in solutions of low molecular weight polyelectrolytes. *Macromolecules.* 22: 4068–4075.

Rotne, J., and S. Prager. 1969. Variational treatment of hydrodynamic interaction in polymers. *J. Chem. Phys.* 50:4831–4837.

Schmitz, K. S. 1990. Dynamic Light Scattering by Macromolecules. Academic Press, New York. 164.

Smith, E. R. 1987. Boundary conditions on hydrodynamics in simulations of dense systems. *Faraday Discuss. Chem. Soc.* 83:193–198.

Smith, E. R., W. van Megen, and I. Snook. 1987. Hydrodynamic interactions in Brownian dynamics. I. Periodic boundary conditions for computer simulations. *Physica A.* 143A:441–467.

Squire, P. G., P. Moser, and C. T. O'Konski. 1968. The hydrodynamic properties of bovine serum albumin monomer and dimer. *Biochemistry.* 7:4261–4272.

Stigter, D. 1977. Interactions of highly charged colloidal cylinders with applications to double-stranded DNA. *Biopolymers.* 16:1435–1448.

Stigter, D. 1979. The ordinary-extraordinary transition of poly(l-lysine-HBr) in NaBr solutions. *Biopolymers.* 18:3125–3127.

Van Megen, W., and I. Snook. 1988. Dynamic computer simulation of concentrated dispersions. *J. Chem. Phys.* 88:1185–1191.

Wang, L., M. M. Garner, M. T. Record, Jr., and H. Yu. 1991. Self-diffusion and cooperative diffusion of a rodlike DNA fragment. *Macromolecules.* 24:2368–2376.

Wattenbarger, M. R., V. A. Bloomfield, Z. Bu, and P. S. Russo. 1992. Diffusion of proteins in DNA solutions. *Macromolecules.* 25: 5263–5265.

Zimmerman, S. B., and A. Minton. 1993. Macromolecular crowding: biochemical, biophysical, and physiological consequences. *Annu. Rev. Biophys. Biomol. Struct.* 22:27–65.